

UNCLASSIFIED

AD

AD-E404 136

Technical Report AREIS-TR-18002

## **PART GEOMETRY CONSIDERATIONS WHEN PERFORMING COMPUTED TOMOGRAPHY**

Stephan C. Zuber

September 2019



U.S. ARMY COMBAT CAPABILITIES DEVELOPMENT  
COMMAND ARMAMENTS CENTER

Enterprise and Systems Integration Center

Picatinny Arsenal, New Jersey

Approved for public release; distribution is unlimited.

UNCLASSIFIED

UNCLASSIFIED

The views, opinions, and/or findings contained in this report are those of the author(s) and should not be construed as an official Department of the Army position, policy, or decision, unless so designated by other documentation.

The citation in this report of the names of commercial firms or commercially available products or services does not constitute official endorsement by or approval of the U.S. Government.

Destroy by any means possible to prevent disclosure of contents or reconstruction of the document. Do not return to the originator.

UNCLASSIFIED

## UNCLASSIFIED

REPORT DOCUMENTATION PAGE				Form Approved OMB No. 0704-01-0188	
<p>The public reporting burden for this collection of information is estimated to average 1 hour per response, including the time for reviewing instructions, searching existing data sources, gathering and maintaining the data needed, and completing and reviewing the collection of information. Send comments regarding this burden estimate or any other aspect of this collection of information, including suggestions for reducing the burden to Department of Defense, Washington Headquarters Services Directorate for Information Operations and Reports (0704-0188), 1215 Jefferson Davis Highway, Suite 1204, Arlington, VA 22202-4302. Respondents should be aware that notwithstanding any other provision of law, no person shall be subject to any penalty for failing to comply with a collection of information if it does not display a currently valid OMB control number.</p> <p><b>PLEASE DO NOT RETURN YOUR FORM TO THE ABOVE ADDRESS.</b></p>					
1. REPORT DATE (DD-MM-YYYY) September 2019		2. REPORT TYPE Final		3. DATES COVERED (From - To)	
4. TITLE AND SUBTITLE  PART GEOMETRY CONSIDERATIONS WHEN PERFORMING COMPUTED TOMOGRAPHY				5a. CONTRACT NUMBER	
				5b. GRANT NUMBER	
				5c. PROGRAM ELEMENT NUMBER	
6. AUTHORS  Stephan C. Zuber				5d. PROJECT NUMBER	
				5e. TASK NUMBER	
				5f. WORK UNIT NUMBER	
7. PERFORMING ORGANIZATION NAME(S) AND ADDRESS(ES) U.S. Army CCDC AC, ESIC Quality Engineering & System Assurance (QE&SA) Directorate (FCDD-ACE-QS) Picatinny Arsenal, NJ 07806-5000				8. PERFORMING ORGANIZATION REPORT NUMBER	
9. SPONSORING/MONITORING AGENCY NAME(S) AND ADDRESS(ES) U.S. Army CCDC AC, ESIC Knowledge & Process Management Office (FCDD-ACE-K) Picatinny Arsenal, NJ 07806-5000				10. SPONSOR/MONITOR'S ACRONYM(S)	
				11. SPONSOR/MONITOR'S REPORT NUMBER(S) Technical Report AREIS-TR-18002	
12. DISTRIBUTION/AVAILABILITY STATEMENT Approved for public release; distribution is unlimited.					
13. SUPPLEMENTARY NOTES					
14. ABSTRACT  The process in setting up an inspection technique using computed tomography (CT) can appear as being intrinsically simplistic. However, in some cases, the part geometry can complicate the method in how to achieve a balance between image quality throughout a volumetric part where symmetry does not exist. As the complexity of an inspection piece increases, additional considerations are needed in order to obtain the best possible information during the acquisition and reconstruction process. The manner in which the part is orientated can have significant impacts in the achieved contrast and spatial resolution components of the data. This paper is designed to provide a general understanding on these impacts and how to assess certain situations or setup consideration prior to finalizing a technique and performing a complete CT examination of the item.					
15. SUBJECT TERMS  Radiography    Computed tomography (CT)    Munitions    X-ray    Nondestructive testing (NDT) Radiographic testing (RT)					
16. SECURITY CLASSIFICATION OF:			17. LIMITATION OF ABSTRACT  SAR	18. NUMBER OF PAGES  27	19a. NAME OF RESPONSIBLE PERSON Stephan Zuber
a. REPORT U	b. ABSTRACT U	c. THIS PAGE U			19b. TELEPHONE NUMBER (Include area code) (973) 724-4130

Standard Form 298 (Rev. 8/98)  
Prescribed by ANSI Std. Z39.18

UNCLASSIFIED



## CONTENTS

	Page
Introduction	1
Concepts of Attenuation in Different Part Setups	1
Overlaying Compromise	4
Additional Considerations	5
Quantative Assessment of a Computed Tomography Phantom Insert	5
Computed Tomography Hole Phantom Insert	5
Spatial Review of the Hole Phantom (Side/Sagittal View)	6
Spatial Review of the Hole Phantom (Top-down/Axial View)	9
Contrast Review of the Hole Phantom	11
Modulation Transfer Function	12
Qualitative Assessment of an Electrical Timer	14
Physical Setup	14
Reconstruction Comparison	14
Conclusions	17
References	19
List of Symbols, Abbreviations, and Acronyms	21
Distribution List	23

## FIGURES

1 Ray traces of photons passing through a vertically positioned (upright) square rod during rotation within a CT acquisition sequence	2
2 Ray traces of photons passing through an upright cylindrical rod during rotation within a CT acquisition sequence	2
3 Ray traces of photons passing through a horizontally positioned square rod during rotation within a CT acquisition sequence	3
4 Photographs showing a CT phantom in two tested part orientations	6
5 Side-view perspective of the CT hole phantom: vertical orientation (x-axis)	7
6 Side view perspective of the CT hole phantom: horizontal orientation (x-axis)	7
7 Line profile measurements (grayscale value versus pixel location) across each set of resolution holes in the side-view perspective of the phantom: horizontal (x-axis) orientation in blue and vertical (x-axis) orientation in orange	8

**FIGURES**  
(continued)

	Page
8 Top-down perspective of the CT phantom	9
9 Line profile measurements (grayscale value versus pixel location) across each set of resolution holes in the top-down perspective of the phantom: horizontal (y-axis) orientation in blue and vertical (z-axis) orientation in orange	10
10 MTF characteristic curves for the two orientations and two slice planes	13
11 Photographs showing the setup of a common electrical timer in the two orientations under examination	14
12 Slice plane A taken from the reconstruction of the timer	15
13 Slice plane B of the timer	16

## INTRODUCTION

The process in which a part or component is placed in between a radiation source and detector for computed tomography (CT) appears as a simplistic step in setting up an inspection. However, in some cases the part may be asymmetric and affect the dose or exposure that reaches the detector during the acquisition cycle where the total attenuation over the field of view (FOV) changes significantly. In other instances, the exterior of the part may be symmetric but the internal components may not be. In which case, the design could drastically affect the exposure in certain regions of interest (ROI) and reduce the number of projections that sufficiently detect or account for the materials inside. As the complexity of an inspection piece increases additional considerations are needed in order to obtain the best possible information during the acquisition and reconstruction process. The manner in which the part is orientated can have significant impacts in the achieved contrast and spatial resolution components of the data. This paper is designed to provide a general understanding on these impacts and how to assess certain situations or setup considerations prior to finalizing a technique and performing a complete CT examination of the product.

## CONCEPTS OF ATTENUATION IN DIFFERENT PART SETUPS

### Paths of Attenuation

The path in which an x-ray photon or series of photons passes through an inspection piece, its total attenuation, and the total amount of radiation that results at the point of conversion within a detector provides the primary information on the quality of an image. Other variables have significant impacts as well such as scatter, initial radiation quality, and beam hardening just to name a few. However, assuming an ideal case, the change in the dose through the part will dictate image quality. This means the manner in which the radiation is passed through the exterior and interior of the part varies the degree of how sensitive the image quality is or can be relative to signal and contrast. Using a basic example, assume there is an elongated square rod that is placed on the rotating turntable of a CT inspection system being prepared for examination. Given that the rod is positioned so that the long axis is vertical (standing upright) and one side of the square is parallel with the detector, the attenuation of any one photon will only vary slightly during the rotation and acquisition of the rod. Figure 1 shows possible ray paths through the square rod during the rotation. If the rod were cylindrical in shape, the attenuation would be the same throughout due to its symmetry, similar to what is shown in figure 2. Now consider the orientation where the square rod was placed horizontally on the turntable where the center of rotation was about the short axis of the inspection piece. This concept can be seen in figure 3 where the range of material thickness varies more drastically than the setup in figure 1.

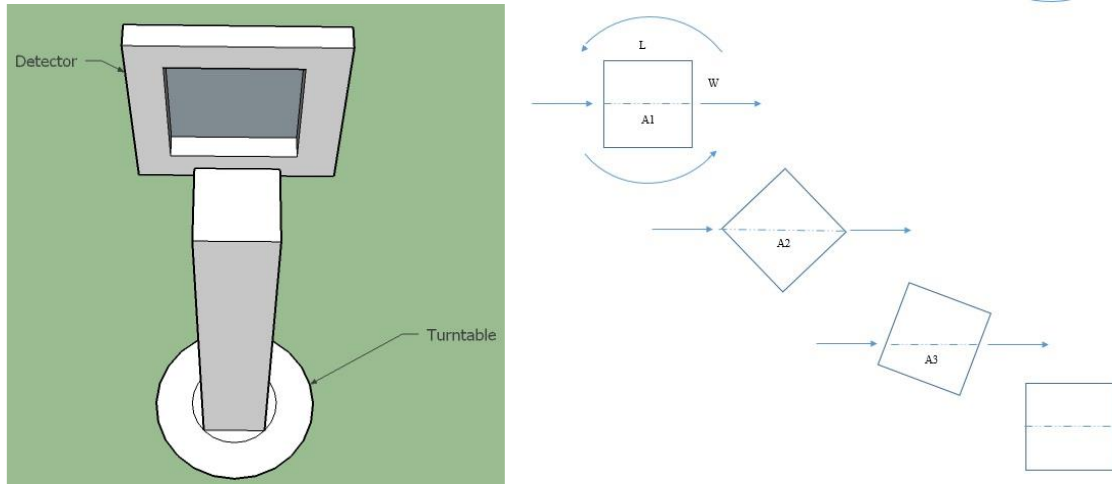


Figure 1  
Ray traces of photons passing through a vertically positioned (upright) square rod during rotation within a CT acquisition sequence

$$\begin{aligned}
 A_1 &= L = W \\
 A_2 &= \sqrt{L^2 + W^2} = \text{maximum attenuation} \\
 A_1 &< A_3 < A_2
 \end{aligned}
 \tag{1}$$

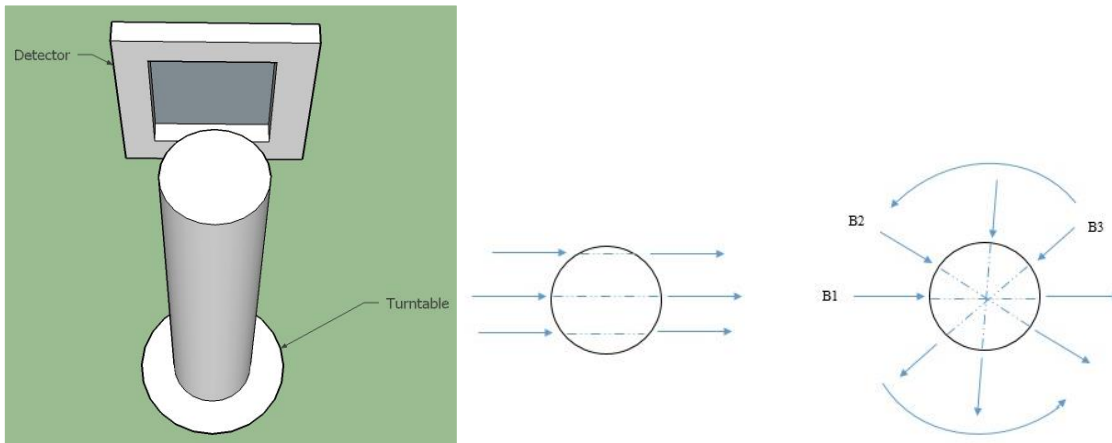


Figure 2  
Ray traces of photons passing through an upright cylindrical rod during rotation within a CT acquisition sequence

$$B_1 = B_2 = B_3 = B_4 \dots \dots
 \tag{2}$$



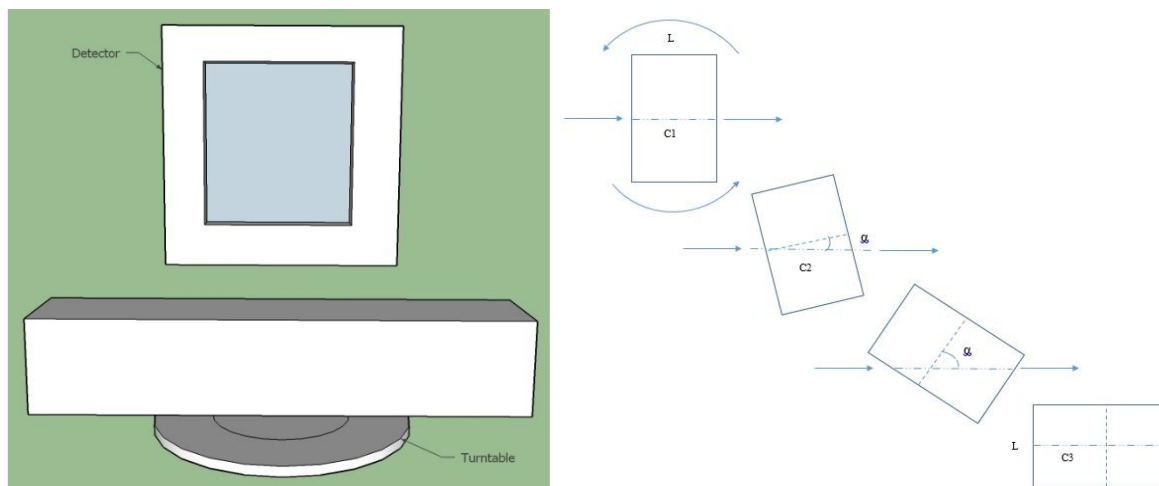


Figure 3

Ray traces of photons passing through a horizontally positioned square rod during rotation within a CT acquisition sequence

$$\begin{aligned} C_1 &= L \\ C_2 &= C_1(1 + \sin(\alpha)), \text{ where } C_2 > C_1 \\ C_3 &\gg C_1 \end{aligned} \quad (3)$$

The purpose of these general examples show that there is a significant number of ways to fixture or orientate a part in order to change the range of attenuation values the detector will see throughout the rotation. Some configurations will be more advantageous than others by reducing the attenuation range while others will be impractical. Factors such as time constraints to design and construct a more complex setup and the availability of a higher penetration or dose needed to adequately saturate the detector are two examples to provide further thought.

Overall, the concepts described so far represent a two-dimensional understanding on the impact the inspection piece shape and its orientation may have on the exposure and resulting reconstruction. However, the same conditions apply three-dimensionally left to right as they do top to bottom and front to back when thinking about the relation of the inspection to the radiation source and detector. The complexity of the issues needed to assess, determine and implement an accurate and fast method to understanding the implications of what options are chosen or employed can be reduced though. The use of the equivalent thickness calculations found in reference 1 can be used to approximate the attenuation of the ray path of a single photon through the highest and lowest attenuating cross section within the inspection piece for the given part orientation. Given the situations previously shown, the user can determine the basic range of equivalent thicknesses that may occur in each projection and resulting reconstruction. This step can be repeated for any given orientation, including tilted subassemblies inside the inspection piece or if assessing whether tilting of the turntable is advantageous. In most situations, only a few of these plug and chug calculations are needed to assure the smallest range through the part is found. In general, this will likely be the position and orientation that will provide the best achievable image quality based on the configuration of the inspection piece. In turn, the user should understand that the physical dimension of length may not be the deciding factor in choosing an orientation. That tends to be a typical habit in industrial radiography primarily stemming from the geometric unsharpness and parallax issues that go along with a two-dimensional overlay.

## Overlaying Compromise

Further complexities arise when a part contains several materials that cause combined attenuation along a ray path. The attenuation overlays the information that is then back-projected across each projection to determine position, size, and specific attenuation (grayscale) values of each component (ref. 2). In certain part designs there may be a substantial number of materials, layers, and angles at which the least amount of attenuation and/or smallest range of attenuation occurs. In these circumstances, the other ideal assumptions on scatter, noise, and energy spectrum shifts have to be assessed. Although the most extreme attenuation ranges can be determined by short hand calculations or with modeling and simulation. Some general rules can be applied that consistently provide a constructive direction to follow in achieving the most practical and optimal radiographic technique:

- Minimize the difference between the minimum and maximum attenuation through the part by flattening the range of contrast produced by the detector (e.g., by using inline beam filters).
- Ensure adequate penetration through the thickest/densest ray path by obtaining a sufficient signal to noise ratio (SNR). If lower attenuation materials become over saturated as a result, additional inline beam filtration can help balance the contrast with the thicker assemblies (refs. 3, 4, 5, and 6).
- Balance the position of the part between being off axis from the centerline rotation of the turntable while not increasing the total open FOV during the rotation. This can be accomplished using shutters, masking, collimation, or a combination of the three.
- Maintain rigid stability of the part during the acquisition cycle to minimize vibration and movement of the part in relation to the system.
- If the part is symmetric on the exterior but is known to have layered materials internally, select the orientation with the smallest maximum attenuation ray path. In some cases, this practice may seem unconventional and result in imaging through the long axis of the part. However, in the assessment section, substantiating evidence will show why this is not always the case.
- In specialized parts such as compact circuitry, use an additional tilt of the rotational table to allow more access to image in-between or around high attenuation regions such as solder joints or precious metal coatings. Care should be taken to balance between gaining ray trace access around these regions and causing a higher total attenuation of the surrounding materials or casing that may reduce the SNR and overall contrast to noise ratio (CNR).
- Use a balance of the smallest spot size while still maintaining the nominal penetration and exposure needed through the part and on the detector. In addition, the total unsharpness, effective resolution, apparent parallax [Feldkamp limit (ref. 2)], contrast resolution, and overall image quality requirements should be verified for conformance.
- If only a portion of the inspection piece is actually under investigation, increase physical magnification such that only the area of interest is within the FOV to increase the relative spacing between layers and overlapping subcomponents.
- Perform a short acquisition and reconstruction in two orthogonal orientations to qualitatively and quantitatively assess if one is better than the other or if another orientation would comprise between them. Perform the hand calculation using the ideal attenuation formula, using the highest attenuator per subassembly as the baseline for each layer within the entire piece, and checking for at least two orthogonal ray traces.

## Additional Considerations

In regard to using rotational table tilt, several other factors and variables have to be taken into account. As a greater angle of tilt is added, the more sound the fixturing is needed to keep the part stabilized. This can sometimes cause issues if the fixturing overlaps the region of interest or causes additional artifacts to occur. Using the tilt option will also cause a larger FOV to be needed since the total circumference (width) of the rotation will be larger. Unless the system in use has a variable collimation device to track with the inspection piece to sustain a constant FOV during the rotation and acquisition cycle, additional noise will occur within the final reconstruction. This is primarily due to the open regions of the FOV allowing more scattered radiation into the image. The added open field may also cause issues when the dose needed to image the part exceeds the saturation limit of the detector. In general, the smaller the FOV, the lower the dose to the detector is and the higher the power can be used to image through the part. This in turn allows greater penetration and/or exposure in the area of interest. In some cases, these characteristics are more important than the added benefits of adding tilt.

When using or discussing helical acquisitions, the constraints to the FOV are also a factor in image quality but primarily in the vertical direction or in the direction of translation across the detector. The best attempt should be made to ensure the beginning and end of the rotation do not contain excessive amounts of open field exposure. Depending on part design and area of interest, sometimes this is unavoidable. However, increasing physical magnification, changing the starting and ending height, and collimating down the FOV can assist in reducing the noise within the final reconstruction. The inherent motion involved in helical CT allows a greater access of photons to travel around the subcomponents of a given assembly. In some cases, the added parallax at the ends of the FOV assist in decreasing the effective attenuation length of the part by transmitting through it on an angle into the detector. Other instances allow optimized alignment of each interface across the mid-plane of the reconstruction. This reduces geometric distortions, artifacts such as beam hardening, and vastly reduces the acquisition time. In the case of this report, the helical method of CT was not reviewed; however, supporting information on the benefits and tradeoffs of using various acquisition techniques in CT can be found within reference 7.

## QUANTATIVE ASSESSMENT OF A COMPUTED TOMOGRAPHY PHANTOM INSERT

### Computed Tomography Hole Phantom Insert

The first example to show the differences in the concepts of different reconstruction outcomes as attributed to the orientation is provided in this section. A standardized CT phantom insert tool was used to quantify the differences in the SNR, CNR, and spatial resolution. The hole sizes in the phantom from largest to smallest are 1.75, 1.5, 1.25, 1.0, 0.75, 0.61, 0.5, 0.4, and 0.2 mm in diameter/thickness. They are listed respectively as 1 through 9 in the following graphical examples. Figure 4 shows photographs of the two orthogonal orientations tested in respect to the x-ray source, detector, and turntable. The centerline of the phantom was placed at approximately the same position for both setups to reduce any variation caused by the polyenergetic beam, gain and offset corrections, and geometric calibrations that carried through the experiment. Additional information on the hole phantom insert under test can be found in reference 7 of this report.

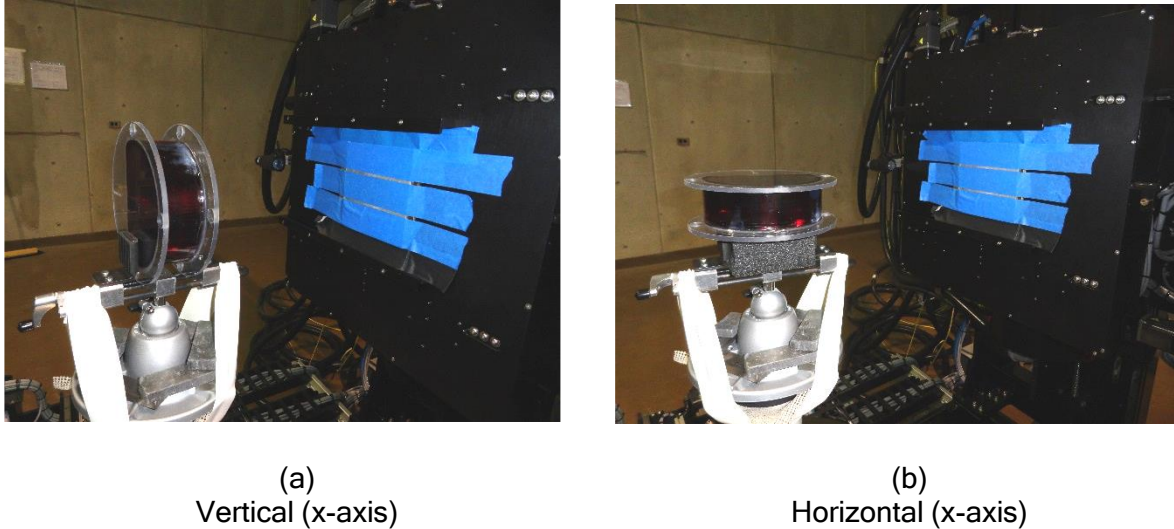


Figure 4  
Photographs showing a CT phantom in two tested part orientations

#### Spatial Review of the Hole Phantom (Side/Sagittal View)

The spatial and contrast resolution of the reconstructions of this report were assessed using several tools including line profiles, SNR, CNR, contrast sensitivity (CS), and modulation transfer function (MTF) measurements in specific ROIs. The first evaluation was performed using a line profile across the long axis of the holes for each set of thicknesses. Figure 5 shows the slice plane for each of the nine sets for the vertical orientation while figure 6 shows the nine sets in the horizontal positioning. The alignment of each slice was completed manually, and the best attempt was made to slice through the center of each hole to assure accuracy of the measurement. In some cases, the entire length of the holes were not visible so the area that most clearly showed the cavities was used. A note to make is that the terms side view and top-down view are used throughout this report for ease of understanding; however, the correct technical terminology is sagittal and axial, respectively.

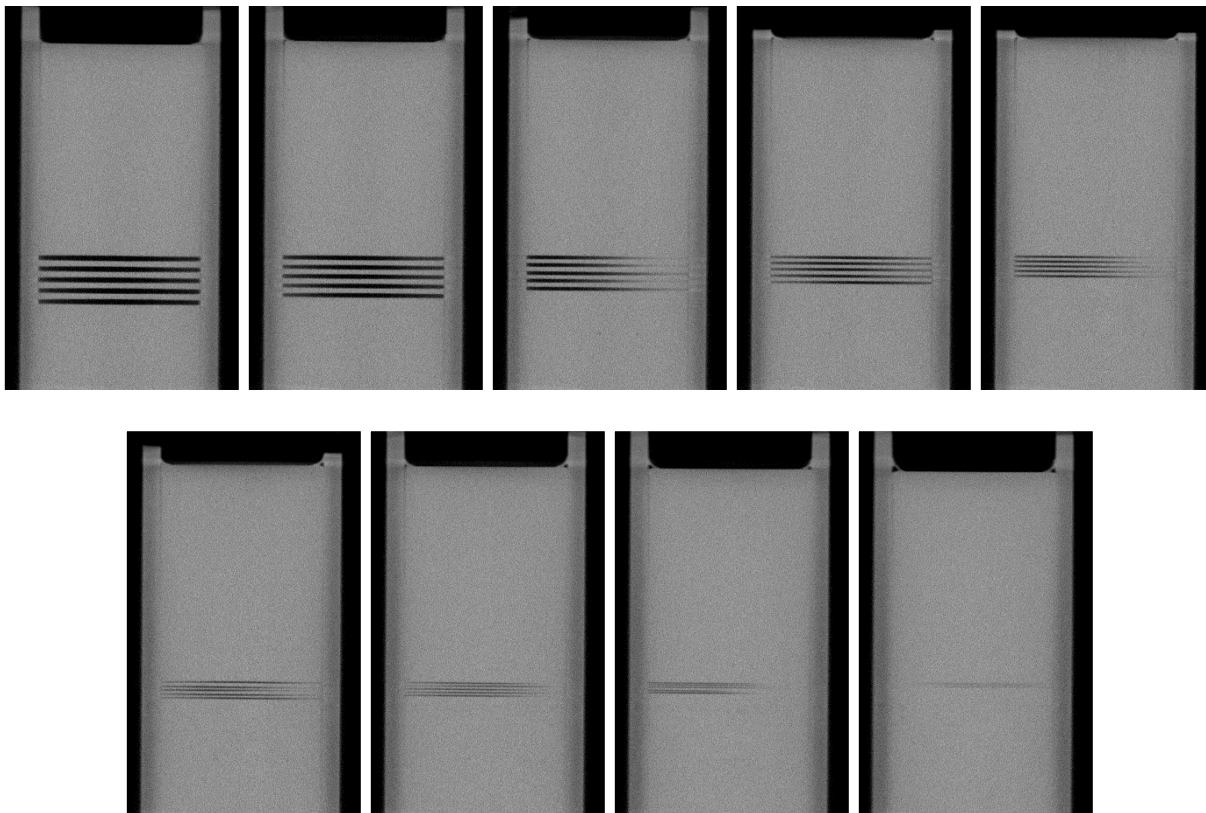


Figure 5  
Side-view perspective of the CT hole phantom: vertical orientation (x-axis)

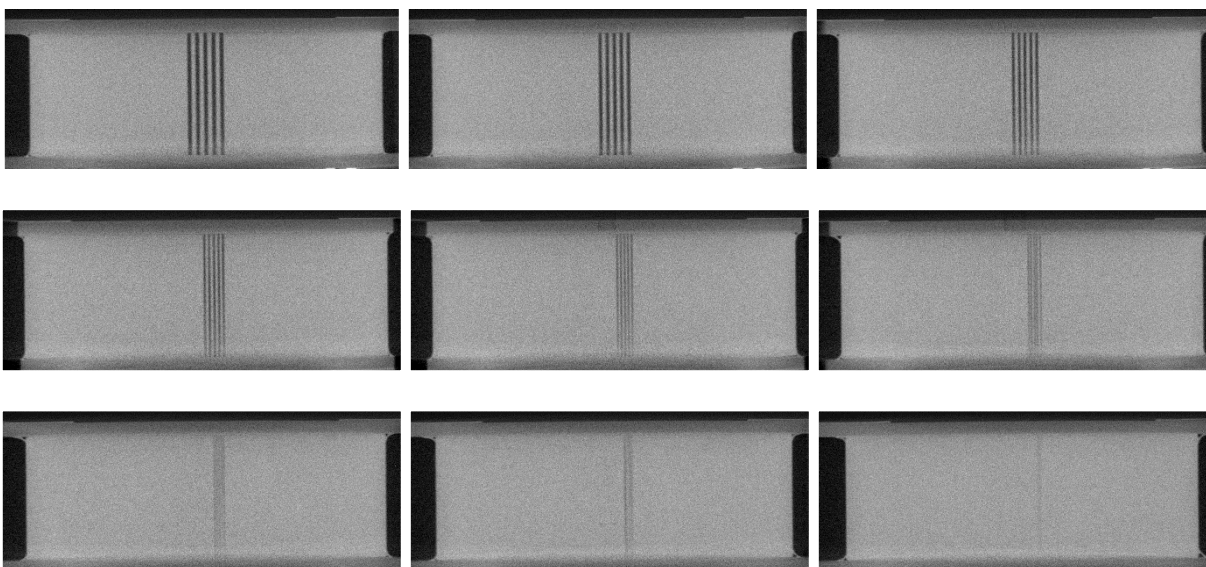


Figure 6  
Side view perspective of the CT hole phantom: horizontal orientation (x-axis)

The graphical plots of the line profiles for the two orientations are shown in figure 7. From this data, it is known that the mean signal obtained through the horizontal orientation and the noise that reduced the detection of the holes past set 7 were higher (0.5 mm). The smoothness of the curves for each hole was also noticeably more inconsistent in the horizontal position, which likely occurred as a result of increased noise and lower contrast between the holes and the interior of the insert in comparison to the vertical setup. Both orientations had limitations reliably detecting the separations below set 7.

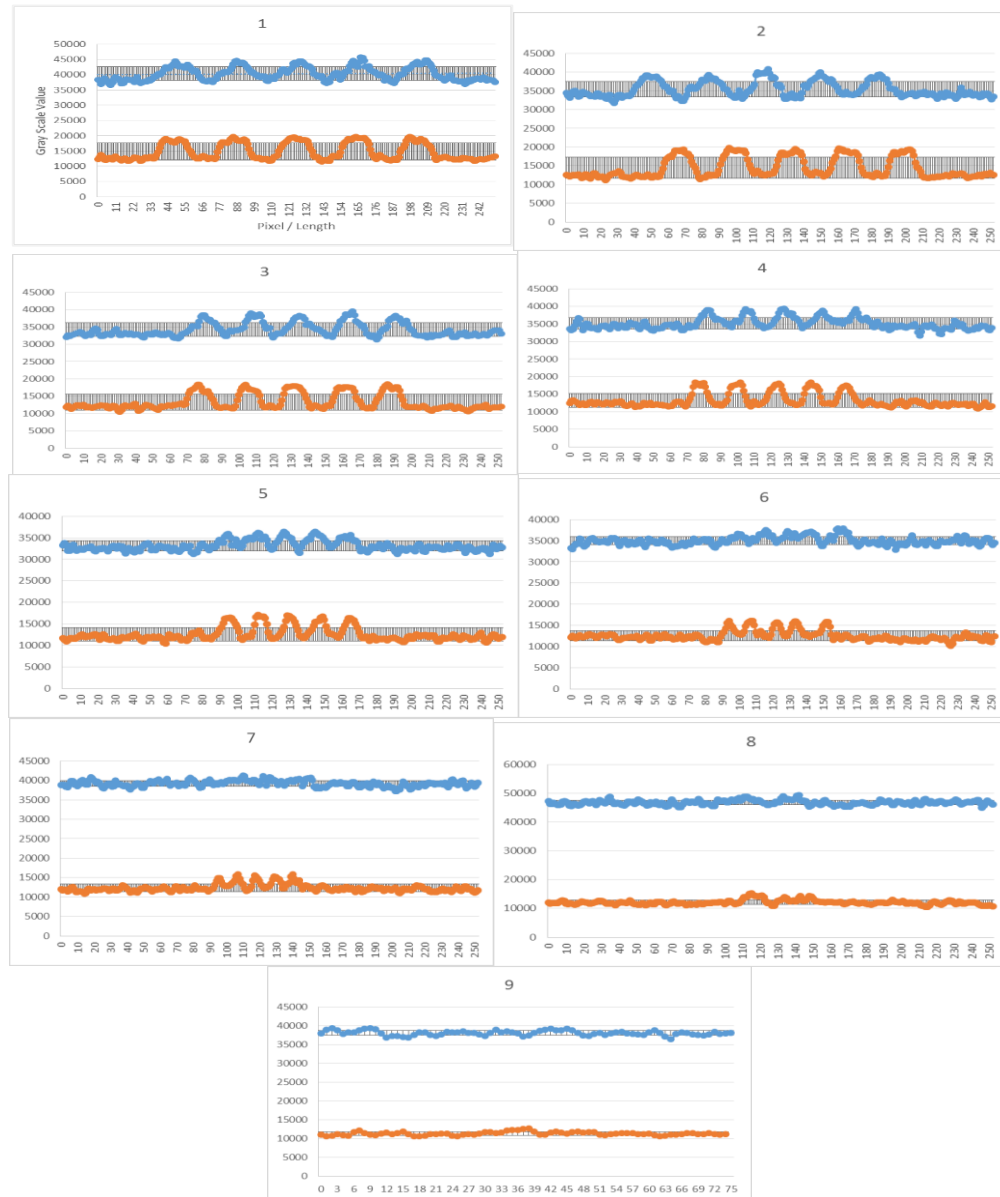


Figure 7

Line profile measurements (grayscale value versus pixel location) across each set of resolution holes in the side-view perspective of the phantom: horizontal (x-axis) orientation in blue and vertical (x-axis) orientation in orange

### Spatial Review of the Hole Phantom (Top-down/Axial View)

For comparison and a more thorough determination of the two reconstructions, line profiles were also taken and plotted using a slice plane through the long axis of the phantom. In this case, the holes are seen in the top-down perspective and the line was drawn down the centerline of each row as close to the true diameter of the holes as possible. Figure 8 presents the reconstruction planes as they were sliced. The standard deviation range is provided to show a basic qualitative way of assuring the holes are truly detected whereas the holes are distinctly detected if the signal reaches beyond the deviation. If the signal was right in line with the magnitude of the noise, the holes are detectable but not consistently, and if the signal was below the noise, the holes were completely undetectable.

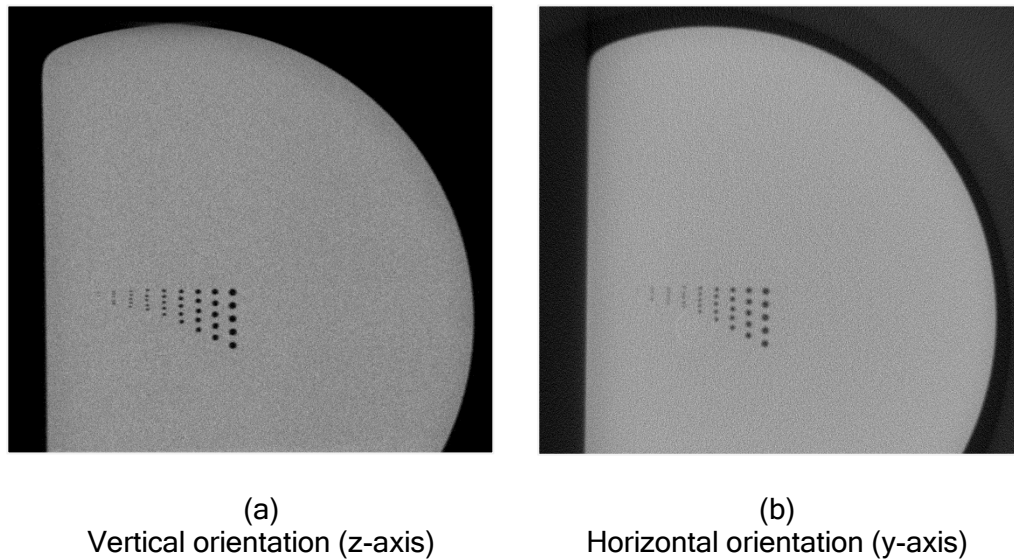


Figure 8  
Top-down perspective of the CT phantom

The data seen within figure 9 shows similar results to the side-view measurements in that both the signal and noise is higher in the horizontal orientation. In addition, the smoothness of the curves is more consistent and the sets of holes in series 6, 7, and 8 (0.61, 0.5, and 0.4 mm, respectively) are only measurable in the vertical setup.



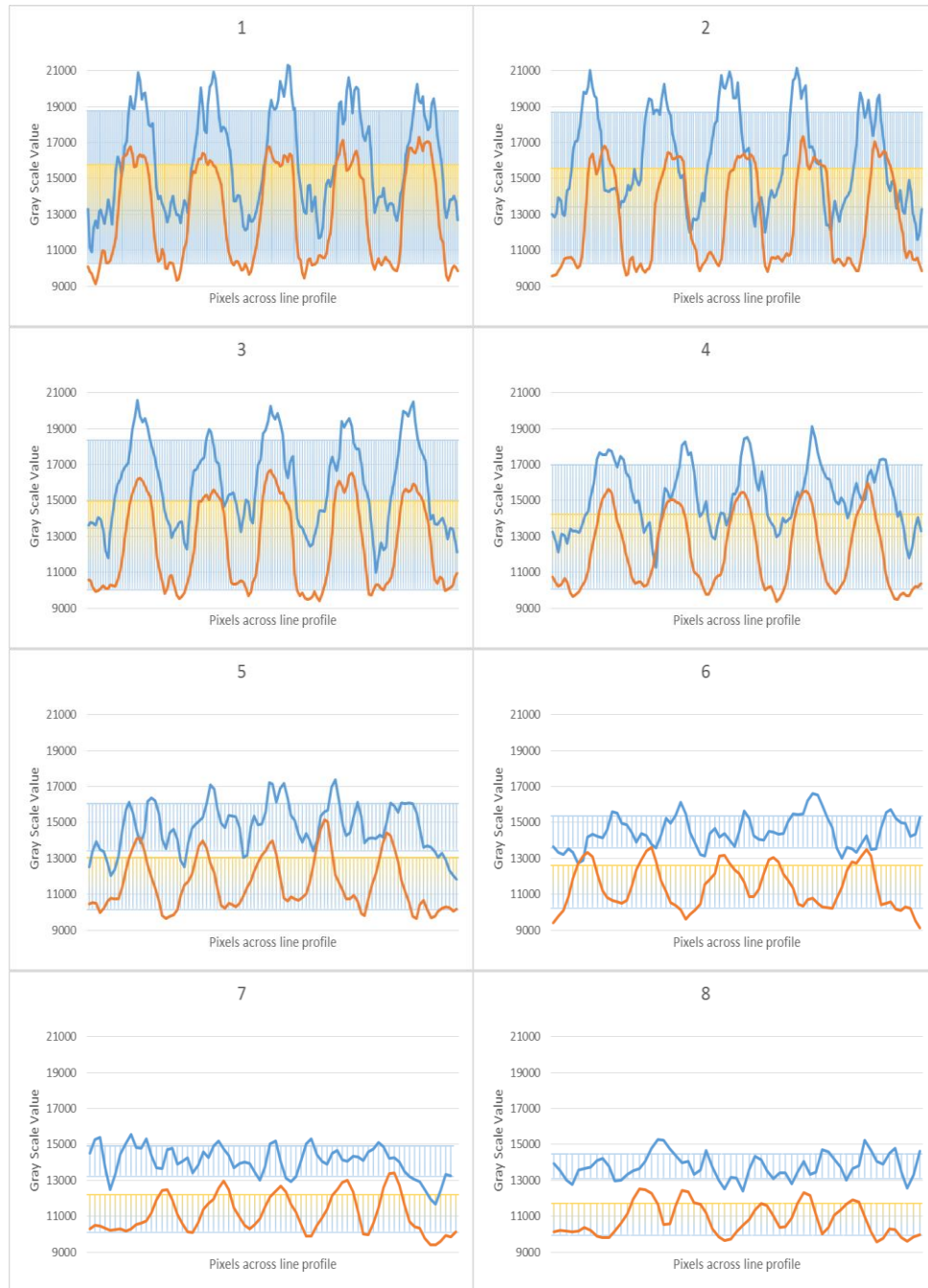


Figure 9

Line profile measurements (grayscale value versus pixel location) across each set of resolution holes in the top-down perspective of the phantom: horizontal (y-axis) orientation in blue and vertical (z-axis) orientation in orange



## Contrast Review of the Hole Phantom

To further compare the two orientations, the signal noise and contrast were measured. Table 1 provides the acquired values of each orientation for both slice planes that were used in the previous section. The ratio of the mean gray value (GV) or signal and standard deviation (SD) or noise within a ROI provides the SNR, which is a quantitative measurement on the quality of the exposure in the selected region. In both slice planes, the vertical orientation had a higher SNR value.

Table 1  
SNR and CNR measurements of the hole phantom and surrounding background

SNR measurements			
Horizontal - side	Signal/mean (GV)	Noise/SD (GV)	SNR
Background	10923.47	508.33	21.49
Area adjacent to holes	18827.27	642.64	29.30
Vertical - side	Signal/mean (GV)	Noise/SD (GV)	SNR
Background	9997.44	369.01	27.09
Area adjacent to holes	17692.80	464.65	38.08
Horizontal - top down	Signal/mean (GV)	Noise/SD (GV)	SNR
Background	12177.67	587.26	20.74
Area adjacent to holes	21698.28	753.18	28.81
Vertical - top down	Signal/mean (GV)	Noise/SD (GV)	SNR
Background	10006.54	326.45	30.65
Area adjacent to holes	17298.76	423.47	40.85
CNR measurements			
Orientation	CNR	CS (%)	
<i>Horizontal - side</i>	15.55	0.72	
<i>Vertical - side</i>	20.85	0.77	
<i>Horizontal - top down</i>	16.21	0.78	
<i>Vertical - top down</i>	22.34	0.73	

The CNR is the ratio of the mean signals of two adjacent ROIs and the noise associated with the background of the exposure. This provides a quantitative measurement of contrast between the two regions, specifically the background and internal material within the phantom. The higher the CNR, the larger the contrast difference is between the two regions. In most cases, this also equates to a larger dynamic range or latitude that is achieved across the materials being imaged. The vertical orientation had higher CNR values across both slice planes. The CS is the ratio of the CNR and SNR and is a general comparative value of what the potential change in material thickness or physical density can be detected between the two ROIs. In this example, the higher the CS is, the larger the measurable contrast difference between those regions is for a given exposure. In the

Approved for public release; distribution is unlimited.

UNCLASSIFIED

side-view slice plane, the vertical orientation showed the best CS while in the top-down plane, the horizontal orientation was slightly better.

### Modulation Transfer Function

Measuring the MTF provides a response curve across a specific interface that correlates into the total resolution of the ROI, typically expressed in cycles per pixel (cy/pixel), pixels per inch (pixels/in.), or inline pairs per millimeter (Lp/mm). Using the same CT hole phantom insert, an additional resolution measurement was taken on the outside of the main housing. The outside of the housing was selected as a ROI where potential variations in contrast and edge sharpness would occur. If there was a critical interface that was under examination, the MTF could also be measured there to ensure repeatable results during multiple tests, baselining the systems response, and for assuring the technique meets the inspection requirements. In the case of the hole phantom, the side wall of one of the holes and the inner material of the insert could be compared; however, for this general comparison, a more ambiguous region was selected. The MTF was performed using the same process described within reference 7. The output curves provided in figure 10 show the MTF responses across the insert for both orientations in both slice planes. The results at 10 and 50% modulation are recorded within table 2 and were determined using the 6th order polynomial trend line-fitted equation. The conversion from cy/pixel to Lp/mm used the voxel size of the reconstruction (88.3  $\mu\text{m}$ ) rather than the pixel width of the detector (200  $\mu\text{m}$ ) to assure more realistic values associated with the effective pixel size for the given physical magnification used (x2.26).

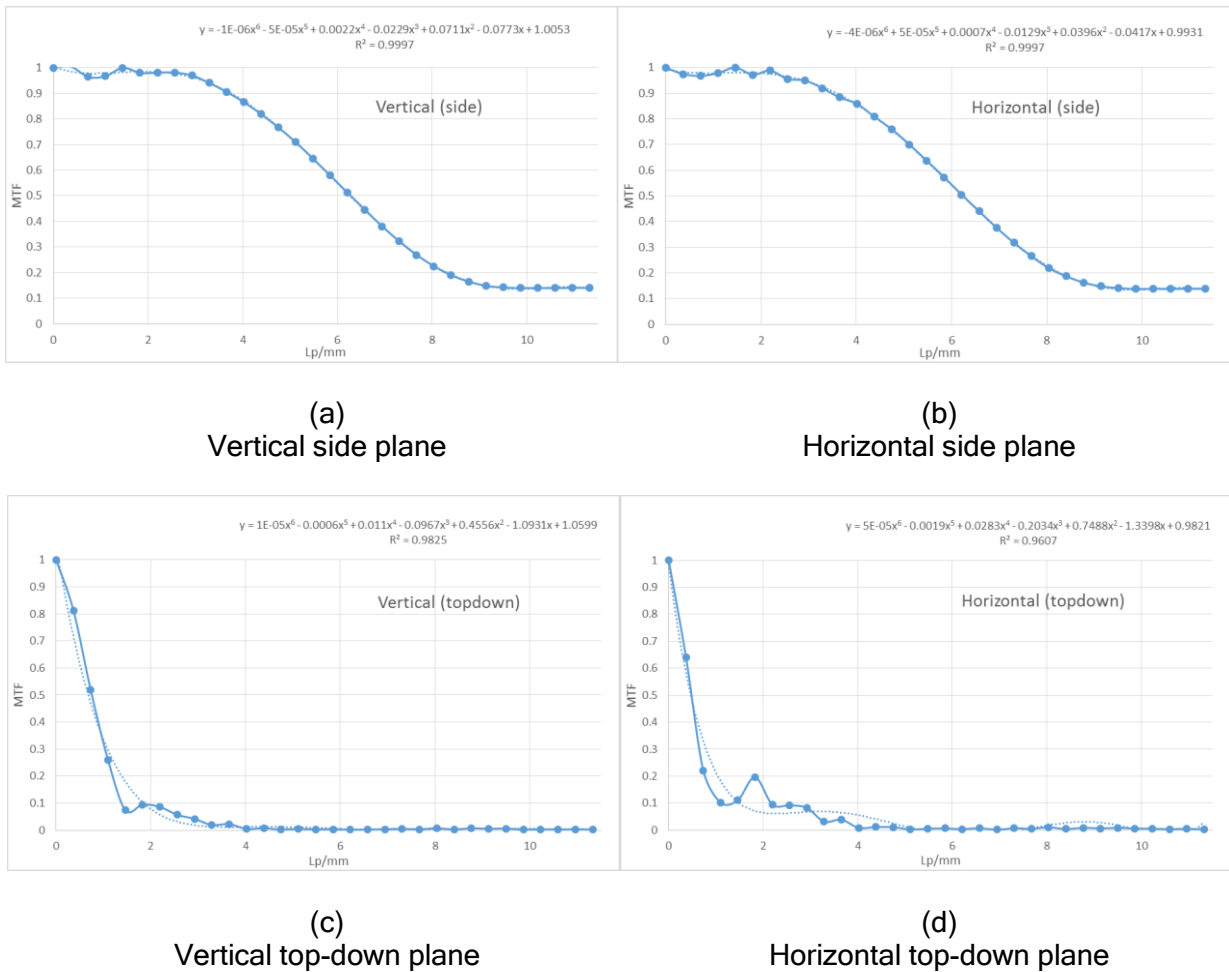


Figure 10  
MTF characteristic curves for the two orientations and two slice planes

Table 2  
MTF values recorded across the outer most edge of the hole phantom insert

50% Modulation			10% Modulation	
<i>Horizontal</i>	<i>Vertical</i>		<i>Horizontal</i>	<i>Vertical</i>
5.96	6.43	Side	NA	NA
0.47	0.68	Top down	1.5	1.85

Overall, the MTF curves for the side views showed high quality results with a relatively small gradient in the descent toward zero modulation. This is indicative of reaching near the diffraction limit or physical constraints of the inspection method for the given inspection piece configuration. However, the MTF curves for the top-down views showed conflicting results where the gradient was quite large in magnitude. This is more in line with noise, artifacts, shifting of the part, and/or other factors during acquisition that would cause the reconstruction to have reduced image quality. In this example, it's primarily caused by a lower than optimized penetration (or dose) through the higher attenuation regions or through the diameter or thickness of the phantom. If a higher SNR was achieved within the interior of the phantom, a higher MTF would be expected. However, given the power limitations on the system in use, this was unavoidable (450kV at 1125W). The extrapolated values of the MTF at 50% modulation consistently verified that the vertical orientation had a better

measure of resolution in both slice planes. The values at 10% modulation also concurred with this conclusion for the top-down slice plane. The side plane MTF curves never reached down to 10% and did not yield a measurement for comparison.

## QUALITATIVE ASSESSMENT OF AN ELECTRICAL TIMER

### Physical Setup

In addition to assessing a known image quality phantom, a basic real world inspection piece was examined to further show the principle impacts that the orientation of the item has on the final reconstruction. In this series of tests, a common off-the-shelf electrical timer was used. This item was selected for the reasoning that it has several functioning subcomponents that are placed in different planes to one another, including completely orthogonal part positions. The process here shows how a part with a common platform of subcomponents and materials can vary the image quality of the inspection. Figure 11 shows photographs of the setup and the two orientations selected for the test. The centerline of the piece was approximately in the same place between the two trials, and both setups used the same correction and calibration files.

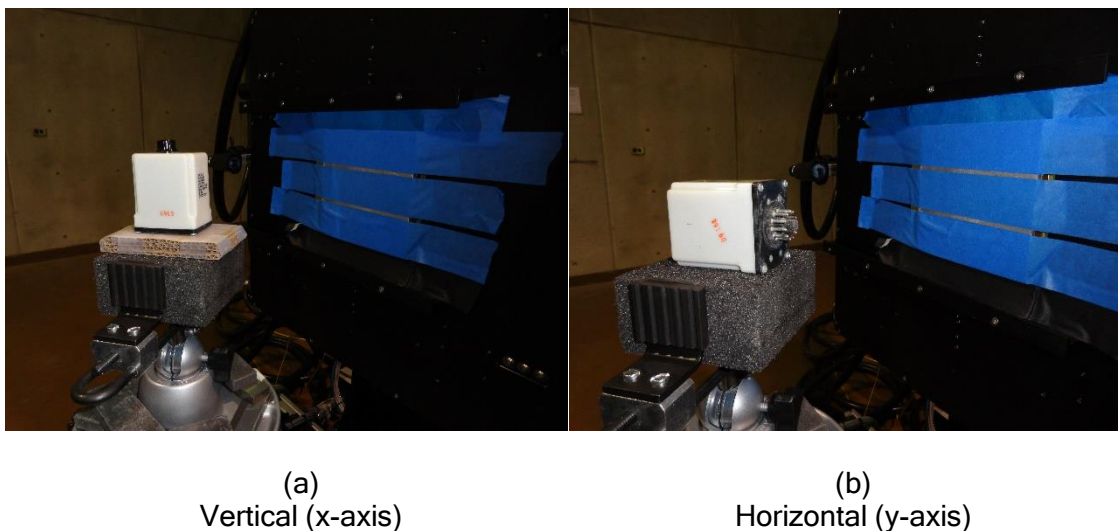


Figure 11  
Photographs showing the setup of a common electrical timer in the two orientations under examination

### Reconstruction Comparison

Once the reconstruction process was completed, slice planes were taken through each orientation at approximately the same place through the timer. From a purely qualitative standpoint and review, the subcomponents that were primarily positioned where their total attenuation was less provided the best contrast and spatial clarity. For example, the images provided in figure 12 show the side and top-down slice plane through a general ROI of the timer for both orientations. It is relatively easy to see that the electrical circuitry seen in the side view is much clearer, higher contrast, and more resolvable in the vertical orientation. The addition of higher attenuation ray paths in the horizontal setup appear to have caused additional noise and artifacts, like beam hardening, to reduce the overall image quality. However, in the top-down slice plane, the mechanical switch and the incoming electrical leads are higher contrast in the horizontal orientation. This example shows some of the subtle variations in image quality that can occur between two different setups for the same piece inspected using the same radiographic technique.

Approved for public release; distribution is unlimited.

UNCLASSIFIED

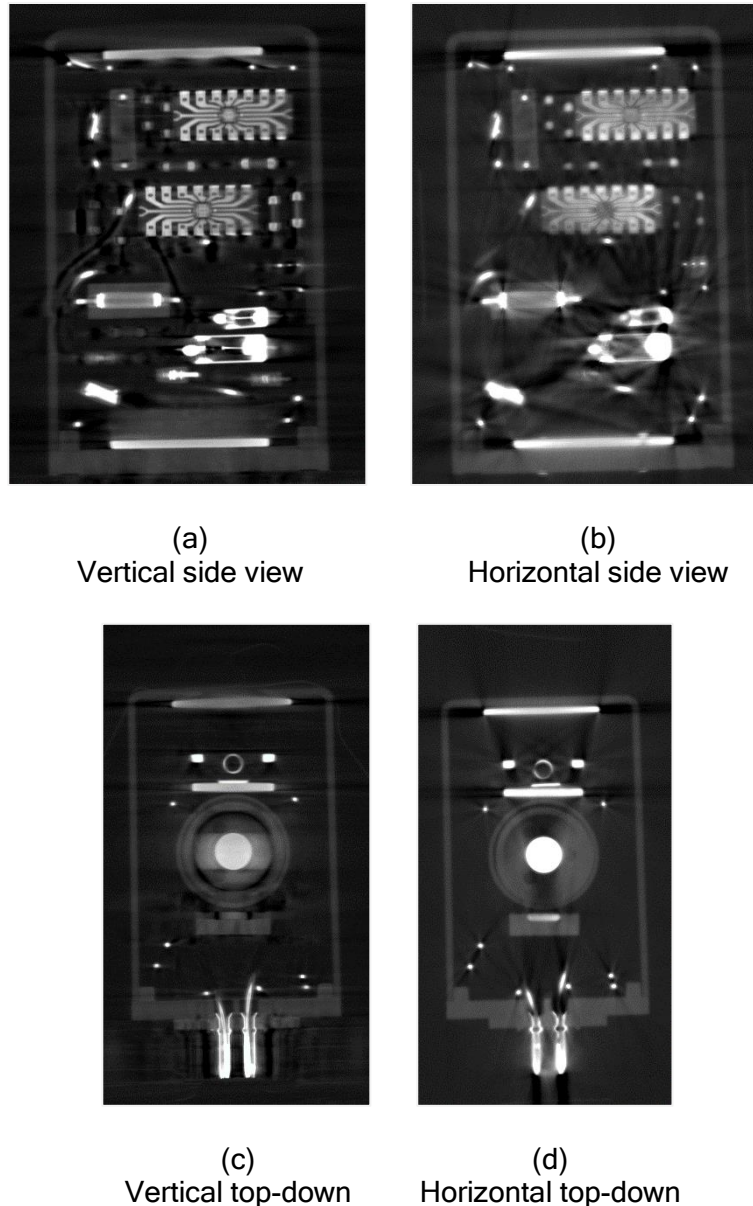
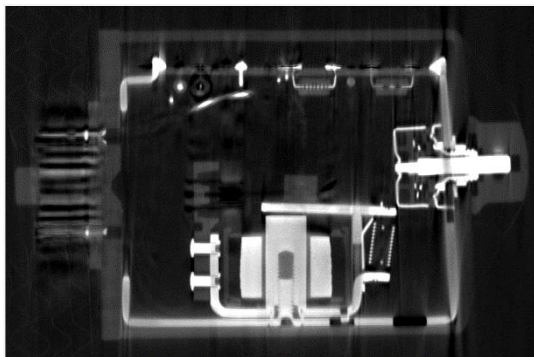
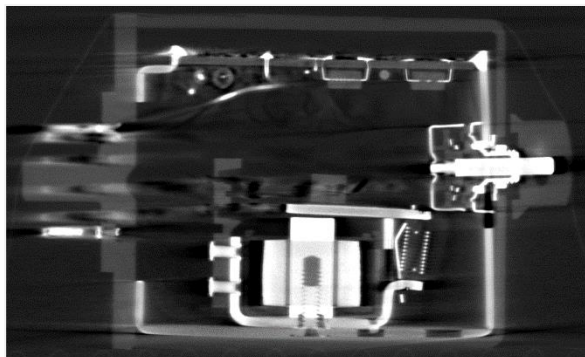


Figure 12  
 Slice plane A taken from the reconstruction of the timer

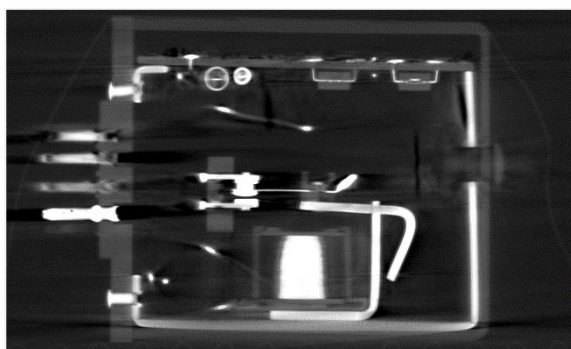
Figure 13 is provided as additional information between the two reconstructions and shows that higher contrast is achieved in the horizontal orientation when viewing the reconstruction from the side-view slice plane and in the vertical orientation when viewing from the top-down perspective. If a quantitative assessment was performed, various tradeoffs would be seen between the two. In some perspectives, views, and projection angles, higher contrast may be needed for cleaner detection of surface interfaces, connections, alignment, and/or overall integrity. On the other hand, the opposing orientation may provide lower contrast and additional artifacts but with an increase in dynamic range across the materials within the sample, which is comprised of tradeoffs that would trace back to the inspection needs, requirements, and intended purpose of the inspection criteria. In certain circumstances like determining part presences, both reconstructions may be acceptable. However, in other situations, the determination of conformance may require the best possible reconstruction that is limited only by the physical constraints of the part itself in order to detect the smallest of details.



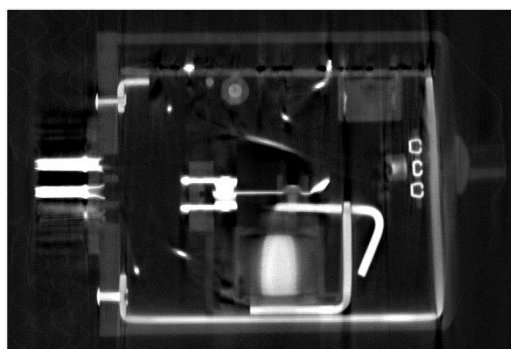
(a)  
Vertical side view



(b)  
Horizontal side view



(c)  
Vertical top-down



(d)  
Horizontal top-down

Figure 13  
Slice plane B of the timer

## CONCLUSIONS

The overall function of this report was to outline several considerations to understand the geometric and physical factors that affect image quality in a computed tomography reconstruction, in regard to the orientation of the inspection piece. Two examples were shown where quantitative and/or qualitative data can determine the significance a different part orientation, configuration, and/or setup can have on the final reconstruction. Given all the other attributes and variables that require thorough knowledge of a volumetric radiographic examination, the orientation of the part can be a critical component even when inspection samples are symmetrical about two axes but geometrically different from each other (for instance, an elongated cylinder, a flattened circuit board, or a planar sheet). When the complexity of a part causes portions of very high attenuation or overlapping materials to be present along the ray path between the radiation source and the detector, several mitigations can be practiced to reduce or even avoid the reduced image quality that may result. General practice in assessing the ray path through a specific design can greatly assist in choosing a particular part orientation and can also increase confidence that the data set will be reliable without having to reacquire using a secondary technique. Several other strategies that were not reviewed in this report include table tilting and helical acquisition sequences. Techniques such as those would have further considerations and constraints but could prove to be an added benefit in specific inspections. Vehicle or body armor systems that can be configured in layered materials of a wide range of physical densities are two such applications. In applications such as these, the bond lines are of significant importance since they dictate the integrity, strength, and function of the design. The major restraint is that they are also a smaller fraction of the total attenuation versus the rest of the assemblies ray path and, therefore, low contrast regions and of lower image quality overall. This is a future area of discussion.





## REFERENCES

1. "Radiography in Modern Industries," Eds. Quinn, R.A. and Sigl, C.C., 4th edition, Eastman Kodak Company, Rochester, NY, 1980.
2. Feldkamp, L.A., Davis, L.C., and Kress, J.W., "Practical Cone Beam Algorithm," Journal of the Optical Society of America A: Optics, Image Science, and Vision, Volume 1, Issue 6, June 1984.
3. "Standard Practice for Radiographic Examination," ASTM E1742/1742M-11, American Society for Testing and Materials, West Conshohocken, PA, 2011.
4. "Standard Practice for Radioscopy," ASTM E1255-09, American Society for Testing and Materials, West Conshohocken, PA, 2009.
5. "Standard Practice for Radiological Examination Using Digital Detector Arrays," ASTM E2698-10, American Society for Testing and Materials, West Conshohocken, PA, 2010.
6. "Standard Practice for Manufacturing Characterization of Digital Detector Arrays," ASTM E2597/2597M-14, American Society for Testing and Materials, West Conshohocken, PA, 2014.
7. Zuber, S., "A Comparative Study on the Characteristics Between Different Computed Tomographic Reconstructions," Materials Evaluation National Journal, pg 1037-1054, American Society of Nondestructive Testing, Columbus, Ohio, July 2016.



LIST OF SYMBOLS, ABBREVIATIONS, AND ACRONYMS

CNR	Contrast to noise ratio
CS	Contrast sensitivity
CT	Computed tomography
cy/pixel	Cycles per pixel
FOV	Field of view
GV	Gray values
in.	inch
kV	kilo-volts, 1E3
Lp/mm	Line pairs per millimeter
m	meter
μm	micro-meter, 1E-6
mm	milli-meter, 1E-3
MTF	Modulation transfer function
ROI	Region of interest
SD	Standard deviation
SNR	Signal to noise ratio
W	Watts



**UNCLASSIFIED**

**DISTRIBUTION LIST**

U.S. Army CCDC AC  
ATTN: FCDD-ACE-K  
FCDD-ACW-FN, S. Zuber  
Picatinny Arsenal, NJ 07806-5000

Defense Technical Information Center (DTIC)  
ATTN: Accessions Division  
8725 John J. Kingman Road, Ste 0944  
Fort Belvoir, VA 22060-6218

GIDEP Operations Center  
P.O. Box 8000  
Corona, CA 91718-8000  
gidep@gidep.org

# UNCLASSIFIED

## REVIEW AND APPROVAL OF ARDEC REPORTS

### THIS IS A:



TECHNICAL REPORT



SPECIAL REPORT



MEMORANDUM REPORT



ARMAMENT GRADUATE SCHOOL REPORT

FUNDING SOURCE N/A

[e.g., TEX3; 6.1 (ILIR, FTAS); 6.2; 6.3; PM funded EMD; PM funded Production/ESIP; Other (please identify)]

### PART GEOMETRY CONSIDERATIONS WHEN PERFORMING COMPUTED TOMOGRAPHY

Title \_\_\_\_\_

Project \_\_\_\_\_

Stephan Zuber  
Author/Project Engineer

Report number/Date received (to be completed by LCSD)

x4130  
Extension

908  
Building

Evaluation Laboratory Division, Radiographic Lab, RDAR-EIQ-EB  
Author's/Project Engineers Office (Division, Laboratory, Symbol)

### PART 1. Must be signed before the report can be edited.

- a. The draft copy of this report has been reviewed for technical accuracy and is approved for editing.
- b. Use Distribution Statement A X, B     , C     , D     , E     , or F      for the reason checked on the continuation of this form. Reason: \_\_\_\_\_
  1. If Statement A is selected, the report will be released to the National Technical Information Service (NTIS) for sale to the general public. Only unclassified reports whose distribution is not limited or controlled in any way are released to NTIS.
  2. If Statement B, C, D, E, or F is selected, the report will be released to the Defense Technical Information Center (DTIC) which will limit distribution according to the conditions indicated in the statement.
- c. The distribution list for this report has been reviewed for accuracy and completeness.

Michael Berry

X

Michael J. Berry  
Chief, Evaluation Laboratory Division

### PART 2. To be signed either when draft report is submitted or after review of reproduction copy.

This report is approved for publication.

Michael Berry

X

Michael J. Berry  
Chief, Evaluation Laboratory Division

RDAR-CIS

(Date)

LCSD 49 supersedes SMCAR Form 49, 20 Dec 06

Approved for public release; distribution is unlimited.

UNCLASSIFIED